



KEK Preprint 2001-11

Belle Preprint 2001-5

# Measurement of Branching Fractions for $B \rightarrow \pi\pi, K\pi$ and $KK$ Decays \*

(The Belle Collaboration)

K. Abe<sup>10</sup>, K. Abe<sup>37</sup>, I. Adachi<sup>10</sup>, Byoung Sup Ahn<sup>15</sup>, H. Aihara<sup>38</sup>, M. Akatsu<sup>20</sup>,  
G. Alimonti<sup>9</sup>, Y. Asano<sup>42</sup>, T. Aso<sup>41</sup>, V. Aulchenko<sup>2</sup>, T. Aushev<sup>13</sup>, A. M. Bakich<sup>34</sup>,  
W. Bartel<sup>6,10</sup>, S. Behari<sup>10</sup>, P. K. Behera<sup>43</sup>, D. Beilina<sup>2</sup>, A. Bondar<sup>2</sup>, A. Bozek<sup>16</sup>,  
T. E. Browder<sup>9</sup>, B. C. K. Casey<sup>9</sup>, P. Chang<sup>24</sup>, Y. Chao<sup>24</sup>, K. F. Chen<sup>24</sup>, B. G. Cheon<sup>33</sup>,  
S.-K. Choi<sup>8</sup>, Y. Choi<sup>33</sup>, S. Eidelman<sup>2</sup>, Y. Enari<sup>20</sup>, R. Enomoto<sup>10,11</sup>, F. Fang<sup>9</sup>, H. Fujii<sup>10</sup>,  
M. Fukushima<sup>11</sup>, A. Garmash<sup>2,10</sup>, A. Gordon<sup>18</sup>, K. Gotow<sup>44</sup>, R. Guo<sup>22</sup>, J. Haba<sup>10</sup>,  
H. Hamasaki<sup>10</sup>, K. Hanagaki<sup>30</sup>, F. Handa<sup>37</sup>, K. Hara<sup>28</sup>, T. Hara<sup>28</sup>, N. C. Hastings<sup>18</sup>,  
H. Hayashii<sup>21</sup>, M. Hazumi<sup>28</sup>, E. M. Heenan<sup>18</sup>, I. Higuchi<sup>37</sup>, T. Higuchi<sup>38</sup>, H. Hirano<sup>40</sup>,  
T. Hojo<sup>28</sup>, Y. Hoshi<sup>36</sup>, W.-S. Hou<sup>24</sup>, S.-C. Hsu<sup>24</sup>, H.-C. Huang<sup>24</sup>, Y. Igarashi<sup>10</sup>, T. Iijima<sup>10†</sup>,  
H. Ikeda<sup>10</sup>, K. Inami<sup>20</sup>, A. Ishikawa<sup>20</sup>, H. Ishino<sup>39</sup>, R. Itoh<sup>10</sup>, G. Iwai<sup>26</sup>, H. Iwasaki<sup>10</sup>,  
Y. Iwasaki<sup>10</sup>, D. J. Jackson<sup>28</sup>, P. Jalocho<sup>16</sup>, H. K. Jang<sup>32</sup>, M. Jones<sup>9</sup>, H. Kakuno<sup>39</sup>,  
J. Kaneko<sup>39</sup>, J. H. Kang<sup>45</sup>, J. S. Kang<sup>15</sup>, N. Katayama<sup>10</sup>, H. Kawai<sup>3</sup>, H. Kawai<sup>38</sup>,  
T. Kawasaki<sup>26</sup>, H. Kichimi<sup>10</sup>, D. W. Kim<sup>33</sup>, Heejong Kim<sup>45</sup>, H. J. Kim<sup>45</sup>, Hyunwoo Kim<sup>15</sup>,  
S. K. Kim<sup>32</sup>, K. Kinoshita<sup>5</sup>, S. Kobayashi<sup>31</sup>, P. Krokovny<sup>2</sup>, R. Kulasiri<sup>5</sup>, S. Kumar<sup>29</sup>,  
A. Kuzmin<sup>2</sup>, Y.-J. Kwon<sup>45</sup>, J. S. Lange<sup>7</sup>, M. H. Lee<sup>10</sup>, S. H. Lee<sup>32</sup>, D. Liventsev<sup>13</sup>,  
R.-S. Lu<sup>24</sup>, D. Marlow<sup>30</sup>, T. Matsubara<sup>38</sup>, S. Matsumoto<sup>4</sup>, T. Matsumoto<sup>20</sup>, Y. Mikami<sup>37</sup>,  
K. Miyabayashi<sup>21</sup>, H. Miyake<sup>28</sup>, H. Miyata<sup>26</sup>, G. R. Moloney<sup>18</sup>, S. Mori<sup>42</sup>, T. Mori<sup>4</sup>,  
A. Murakami<sup>31</sup>, T. Nagamine<sup>37</sup>, Y. Nagasaka<sup>19</sup>, T. Nakadaira<sup>38</sup>, E. Nakano<sup>27</sup>, M. Nakao<sup>10</sup>,  
J. W. Nam<sup>33</sup>, S. Narita<sup>37</sup>, S. Nishida<sup>17</sup>, O. Nitoh<sup>40</sup>, S. Noguchi<sup>21</sup>, T. Nozaki<sup>10</sup>, S. Ogawa<sup>35</sup>,  
T. Ohshima<sup>20</sup>, T. Okabe<sup>20</sup>, S. Okuno<sup>14</sup>, S. L. Olsen<sup>9</sup>, H. Ozaki<sup>10</sup>, P. Pakhlov<sup>13</sup>, H. Palka<sup>16</sup>,  
C. S. Park<sup>32</sup>, C. W. Park<sup>15</sup>, H. Park<sup>15</sup>, L. S. Peak<sup>34</sup>, M. Peters<sup>9</sup>, L. E. Pilonen<sup>44</sup>,  
J. L. Rodriguez<sup>9</sup>, N. Root<sup>2</sup>, M. Rozanska<sup>16</sup>, K. Rybicki<sup>16</sup>, J. Ryuko<sup>28</sup>, H. Sagawa<sup>10</sup>,

---

\*submitted to PRL

†e-mail: toru.iijima@kek.jp

Y. Sakai<sup>10</sup>, H. Sakamoto<sup>17</sup>, M. Satpathy<sup>43</sup>, A. Satpathy<sup>10,5</sup>, S. Schrenk<sup>5</sup>, S. Semenov<sup>13</sup>,  
 K. Senyo<sup>20</sup>, M. E. Sevier<sup>18</sup>, H. Shibuya<sup>35</sup>, B. Shwartz<sup>2</sup>, V. Sidorov<sup>2</sup>, J.B. Singh<sup>29</sup>,  
 S. Stanič<sup>42</sup>, A. Sugi<sup>20</sup>, A. Sugiyama<sup>20</sup>, K. Sumisawa<sup>28</sup>, T. Sumiyoshi<sup>10</sup>, J.-I. Suzuki<sup>10</sup>,  
 K. Suzuki<sup>3†</sup>, S. Suzuki<sup>20</sup>, S. Y. Suzuki<sup>10</sup>, S. K. Swain<sup>9</sup>, H. Tajima<sup>38</sup>, T. Takahashi<sup>27</sup>,  
 F. Takasaki<sup>10</sup>, M. Takita<sup>28</sup>, K. Tamai<sup>10</sup>, N. Tamura<sup>26</sup>, J. Tanaka<sup>38</sup>, M. Tanaka<sup>10</sup>,  
 G. N. Taylor<sup>18</sup>, Y. Teramoto<sup>27</sup>, M. Tomoto<sup>20</sup>, T. Tomura<sup>38</sup>, S. N. Tovey<sup>18</sup>, K. Trabelsi<sup>9</sup>,  
 T. Tsuboyama<sup>10</sup>, T. Tsukamoto<sup>10</sup>, S. Uehara<sup>10</sup>, K. Ueno<sup>24</sup>, Y. Unno<sup>3</sup>, S. Uno<sup>10</sup>,  
 Y. Ushiroda<sup>17,10</sup>, Y. Usov<sup>2</sup>, S. E. Vahsen<sup>30</sup>, G. Varner<sup>9</sup>, K. E. Varvell<sup>34</sup>, C. C. Wang<sup>24</sup>,  
 C. H. Wang<sup>23</sup>, J. G. Wang<sup>44</sup>, M.-Z. Wang<sup>24</sup>, Y. Watanabe<sup>39</sup>, E. Won<sup>32</sup>, B. D. Yabsley<sup>10</sup>,  
 Y. Yamada<sup>10</sup>, M. Yamaga<sup>37</sup>, A. Yamaguchi<sup>37</sup>, H. Yamamoto<sup>9</sup>, Y. Yamashita<sup>25</sup>,  
 M. Yamauchi<sup>10</sup>, S. Yanaka<sup>39</sup>, M. Yokoyama<sup>38</sup>, Y. Yusa<sup>37</sup>, H. Yuta<sup>1</sup>, C.C. Zhang<sup>12</sup>,  
 J. Zhang<sup>42</sup>, H. W. Zhao<sup>10</sup>, Y. Zheng<sup>9</sup>, V. Zhilich<sup>2</sup>, and D. Žontar<sup>42</sup>

<sup>1</sup>Aomori University, Aomori

<sup>2</sup>Budker Institute of Nuclear Physics, Novosibirsk

<sup>3</sup>Chiba University, Chiba

<sup>4</sup>Chuo University, Tokyo

<sup>5</sup>University of Cincinnati, Cincinnati, OH

<sup>6</sup>Deutsches Elektronen-Synchrotron, Hamburg

<sup>7</sup>University of Frankfurt, Frankfurt

<sup>8</sup>Gyeongsang National University, Chinju

<sup>9</sup>University of Hawaii, Honolulu HI

<sup>10</sup>High Energy Accelerator Research Organization (KEK), Tsukuba

<sup>11</sup>Institute for Cosmic Ray Research, University of Tokyo, Tokyo

<sup>12</sup>Institute of High Energy Physics, Chinese Academy of Sciences, Beijing

<sup>13</sup>Institute for Theoretical and Experimental Physics, Moscow

<sup>14</sup>Kanagawa University, Yokohama

<sup>15</sup>Korea University, Seoul

<sup>16</sup>H. Niewodniczanski Institute of Nuclear Physics, Krakow

<sup>17</sup>Kyoto University, Kyoto

<sup>18</sup>University of Melbourne, Victoria

<sup>19</sup>Nagasaki Institute of Applied Science, Nagasaki

<sup>20</sup>Nagoya University, Nagoya

<sup>21</sup>Nara Women's University, Nara

<sup>22</sup>National Kaohsiung Normal University, Kaohsiung

<sup>23</sup>National Lien-Ho Institute of Technology, Miao Li

---

<sup>†</sup>e-mail: kazuhito@bmail.kek.jp

- <sup>24</sup>National Taiwan University, Taipei  
<sup>25</sup>Nihon Dental College, Niigata  
<sup>26</sup>Niigata University, Niigata  
<sup>27</sup>Osaka City University, Osaka  
<sup>28</sup>Osaka University, Osaka  
<sup>29</sup>Panjab University, Chandigarh  
<sup>30</sup>Princeton University, Princeton NJ  
<sup>31</sup>Saga University, Saga  
<sup>32</sup>Seoul National University, Seoul  
<sup>33</sup>Sungkyunkwan University, Suwon  
<sup>34</sup>University of Sydney, Sydney NSW  
<sup>35</sup>Toho University, Funabashi  
<sup>36</sup>Tohoku Gakuin University, Tagajo  
<sup>37</sup>Tohoku University, Sendai  
<sup>38</sup>University of Tokyo, Tokyo  
<sup>39</sup>Tokyo Institute of Technology, Tokyo  
<sup>40</sup>Tokyo University of Agriculture and Technology, Tokyo  
<sup>41</sup>Toyama National College of Maritime Technology, Toyama  
<sup>42</sup>University of Tsukuba, Tsukuba  
<sup>43</sup>Utkal University, Bhubaneswer  
<sup>44</sup>Virginia Polytechnic Institute and State University, Blacksburg VA  
<sup>45</sup>Yonsei University, Seoul

### Abstract

We report measurements of the branching fractions for  $B^0 \rightarrow \pi^+\pi^-$ ,  $K^+\pi^-$ ,  $K^+K^-$  and  $K^0\pi^0$ , and  $B^+ \rightarrow \pi^+\pi^0$ ,  $K^+\pi^0$ ,  $K^0\pi^+$  and  $K^+\bar{K}^0$ . The results are based on  $10.4 \text{ fb}^{-1}$  of data collected on the  $\Upsilon(4S)$  resonance at the KEKB  $e^+e^-$  storage ring with the Belle detector, equipped with a high momentum particle identification system for clear separation of charged  $\pi$  and  $K$  mesons. We find  $\mathcal{B}(B^0 \rightarrow \pi^+\pi^-) = (0.56_{-0.20}^{+0.23} \pm 0.04) \times 10^{-5}$ ,  $\mathcal{B}(B^0 \rightarrow K^+\pi^-) = (1.93_{-0.32}^{+0.34} {}_{-0.06}^{+0.15}) \times 10^{-5}$ ,  $\mathcal{B}(B^+ \rightarrow K^+\pi^0) = (1.63_{-0.33}^{+0.35} {}_{-0.18}^{+0.16}) \times 10^{-5}$ ,  $\mathcal{B}(B^+ \rightarrow K^0\pi^+) = (1.37_{-0.48}^{+0.57} {}_{-0.18}^{+0.19}) \times 10^{-5}$ , and  $\mathcal{B}(B^0 \rightarrow K^0\pi^0) = (1.60_{-0.59}^{+0.72} {}_{-0.27}^{+0.25}) \times 10^{-5}$ , where the first and second errors are statistical and systematic. We also set upper limits of  $\mathcal{B}(B^+ \rightarrow \pi^+\pi^0) < 1.34 \times 10^{-5}$ ,  $\mathcal{B}(B^0 \rightarrow K^+K^-) < 0.27 \times 10^{-5}$ , and  $\mathcal{B}(B^+ \rightarrow K^+\bar{K}^0) < 0.50 \times 10^{-5}$  at the 90% confidence level.

PACS numbers: 13.25.Hw, 14.40.Nd

The charmless hadronic  $B$  decays  $B \rightarrow \pi\pi$ ,  $K\pi$  and  $KK$  provide a rich sample to test the standard model and to probe new physics [1]. Of particular interest are indirect and direct  $CP$  violation in the  $\pi\pi$  and  $K\pi$  modes, which are related to the angles  $\phi_2$  and  $\phi_3$  of the unitarity triangle, respectively [1]. Measurements of branching fractions of these decay modes are an important first step toward these  $CP$  violation studies. However, experimental information is rather limited, and the only published results come from one experiment [2]. One of the key experimental issues is the particle identification (PID) for separation of the high momentum charged  $\pi$  and  $K$  mesons. This is one of the primary reasons that the  $B$  factory experiments [3,4] have been equipped with specialized high momentum PID devices.

In this paper, we report the first results of the Belle experiment on charmless hadronic two-body  $B$  decays into  $\pi\pi$ ,  $K\pi$  and  $KK$  final states. The decay modes studied are  $\pi^+\pi^-$ ,  $K^+\pi^-$ ,  $K^+K^-$  and  $K^0\pi^0$  for  $B^0$  decays, and  $\pi^+\pi^0$ ,  $K^+\pi^0$ ,  $K^0\pi^+$ ,  $K^+\bar{K}^0$ , for  $B^+$  decays. For the modes with  $K^0$  mesons, only  $K_S^0 \rightarrow \pi^+\pi^-$  decays are used. Throughout this paper, the inclusion of charge conjugate states is implied. The results are based on data taken by the Belle detector [5] at the KEKB asymmetric  $e^+e^-$  storage ring [6]. The Belle detector is equipped with aerogel Čerenkov counters (ACC) configured for high momentum PID. The data set consists of  $10.4 \text{ fb}^{-1}$  data taken at the  $\Upsilon(4S)$  resonance, corresponding to 11.1 million  $B\bar{B}$  events, and  $0.6 \text{ fb}^{-1}$  data taken at an energy  $\sim 60 \text{ MeV}$  below the resonance, for systematic studies of the continuum  $q\bar{q}$  background.

Primary charged tracks are required to satisfy track quality cuts based on their impact parameters relative to the interaction point (IP).  $K_S^0$  mesons are reconstructed using pairs of charged tracks that have an invariant mass within  $\pm 30 \text{ MeV}/c^2$  of the known  $K_S^0$  mass and a well reconstructed vertex that is displaced from the IP. Candidate  $\pi^0$  mesons are reconstructed using  $\gamma$  pairs with an invariant mass within  $\pm 16 \text{ MeV}/c^2$  of the nominal  $\pi^0$  mass. The  $B$  meson candidates are reconstructed using the beam constrained mass,  $m_{bc} = \sqrt{E_{\text{beam}}^2 - p_B^2}$ , and the energy difference,  $\Delta E = E_B - E_{\text{beam}}$ , where  $E_{\text{beam}} \equiv \sqrt{s}/2 \simeq 5.290 \text{ GeV}$ , and  $p_B$  and  $E_B$  are the momentum and energy of the reconstructed  $B$  in the  $\Upsilon(4S)$  rest frame, respectively. The signal region for each variable is defined as  $\pm 3\sigma$  from its central value. The resolution in  $m_{bc}$  is dominated by the beam energy spread and is typically  $2.7 \text{ MeV}/c^2$ . The  $\Delta E$  resolution ranges from 20 to 25 MeV, depending on the momentum and energy resolutions for each particle. Normally we compute  $\Delta E$  assuming a  $\pi$  mass for each charged particle. This shifts  $\Delta E$  downward by 44 MeV for each charged  $K$  meson, giving kinematic separation between the  $h\pi^+$  and  $hK^+$  ( $h = \pi, K$ ) final states. In modes with  $\pi^0$  mesons, both the  $m_{bc}$  and  $\Delta E$  distributions are asymmetric due to  $\gamma$  interactions in the material in front of the calorimeter and energy leakage out of the calorimeter. We accept events in the region  $m_{bc} > 5.2 \text{ GeV}/c^2$  and  $|\Delta E| < 0.25 \text{ GeV}$  for the  $h^+h^-$  and  $K_S^0 h^+$  modes, and  $-0.45 < \Delta E < 0.15 \text{ GeV}$  for the  $h^+\pi^0$  and  $K_S^0\pi^0$  modes. In this kinematic window, the

area outside the signal region is defined as a sideband. The signal reconstruction efficiencies after the kinematic window cut are 65% for  $h^+h^-$ , 33% for  $K_S^0h^+$ , 50% for  $h^+\pi^0$ , and 24% for  $K_S^0\pi^0$ , according to a GEANT [7] based Monte Carlo (MC) simulation. The MC tracking efficiency is verified by detailed studies using high momentum tracks from  $D$ ,  $\eta$  and  $K^*$  decays. The reconstruction efficiencies for high momentum  $K_S^0$  and  $\pi^0$  mesons are tested by comparing the ratio of the yield of  $D^+ \rightarrow K_S^0\pi^+$  to  $D^+ \rightarrow K^-\pi^+\pi^+$  and  $D^0 \rightarrow K^-\pi^+\pi^0$  to  $D^0 \rightarrow K^-\pi^+$ , respectively, between data and MC simulation. From these studies, we assign a relative systematic error in these efficiencies of 2.3% per charged track, 12% per  $K_S^0$  and 8.5% per  $\pi^0$  meson.

The background from  $b \rightarrow c$  transitions is negligible. The dominant background is from the continuum  $q\bar{q}$  process. We suppress this background using the event topology, which is spherical for  $B\bar{B}$  events and jet-like for  $q\bar{q}$  events in the  $\Upsilon(4S)$  rest frame. This difference can be quantified by using several variables including the event sphericity,  $S$ , the angle between the  $B$  candidate thrust axis and the thrust axis of the rest of the event,  $\theta_T$ , and the Fox-Wolfram moments [8]  $H_l = \sum_{i,j} |\vec{p}_i||\vec{p}_j|P_l(\cos\theta_{ij})$ , where the indices  $i$  and  $j$  run over all final state particles,  $\vec{p}_i$  and  $\vec{p}_j$  are the momentum vectors of particles  $i$  and  $j$ ,  $P_l$  is the  $l$ -th Legendre polynomial, and  $\theta_{ij}$  is the angle between particles  $i$  and  $j$ . We can also use the  $B$  flight direction,  $\theta_B$ , and the decay axis direction,  $\theta_{hh}$ , which distinguish  $B\bar{B}$  from  $q\bar{q}$  processes based on initial state angular momentum.

We increase the suppression power of the normalized Fox-Wolfram moments,  $R_l = H_l/H_0$ , by decomposing them into three terms:  $R_l = R_l^{ss} + R_l^{so} + R_l^{oo} = (H_l^{ss} + H_l^{so} + H_l^{oo})/H_0$ , where the indices  $ss$ ,  $so$ , and  $oo$  indicate respectively that both, one, or neither of the particles comes from a  $B$  candidate. These are combined into a six term Fisher discriminant [9] called the Super Fox-Wolfram [10] defined as  $SFW = \sum_{l=1}^4 (\alpha_l R_l^{so} + \beta_l R_l^{oo})$ , where  $\alpha_l$  and  $\beta_l$  are Fisher coefficients and  $l=2,4$  for  $\alpha_l$  and  $R_l^{so}$ . The terms  $R_l^{ss}$  and  $R_{l=1,3}^{so}$  are excluded because they are strongly correlated with  $m_{bc}$  and  $\Delta E$ . In the  $h^+h^-$  modes, for example,  $SFW$  gives a 20% increase in the expected significance compared to  $R_2$ .

We combine different  $q\bar{q}$  suppression variables into a single likelihood,  $\mathcal{L}_{s(q\bar{q})} = \prod_i \mathcal{L}_{s(q\bar{q})}^i$ , where the  $\mathcal{L}_{s(q\bar{q})}^i$  denotes the signal( $q\bar{q}$ ) likelihood of the suppression variable  $i$ , and select candidate events by cutting on the likelihood ratio  $\mathcal{R}_s = \mathcal{L}_s/(\mathcal{L}_s + \mathcal{L}_{q\bar{q}})$ . For  $h^+h^-$  and  $K_S^0h^+$ , the likelihood contains  $SFW$ ,  $\cos\theta_B$ , and  $\cos\theta_{hh}$ . In modes with  $\pi^0$  mesons, the  $q\bar{q}$  background is significantly larger. In this case, we first make a loose cut on  $\cos\theta_T$ . Next, we extend  $SFW$  to include  $\cos\theta_T$  and  $S$ , and form the likelihood using this extended  $SFW$  and  $\cos\theta_B$ . In each case, the signal probability density functions (PDFs) are determined using MC simulation and the  $q\bar{q}$  PDFs are taken from  $m_{bc}$  sideband data. The performance of  $\mathcal{R}_s$  varies among the modes with efficiencies ranging from 40% to 51% while removing more than 95% of the  $q\bar{q}$  background. The  $\pi^+\pi^0$  mode calls for a tighter cut with an efficiency of 26%. The error in these efficiencies is determined by applying the same procedure to the

$B^+ \rightarrow \bar{D}^0\pi^+$ ,  $\bar{D}^0 \rightarrow K^-\pi^+$  event sample and comparing the cut efficiencies between data and MC. The relative systematic error is determined to be 4%.

The high momentum charged  $\pi$  and  $K$  mesons ( $1.5 < p_{h\pm} < 4.5$  GeV/ $c$  in the laboratory frame) are distinguished by cutting on the  $\pi(K)$  likelihood ratio  $\mathcal{R}_{\pi(K)} \equiv \mathcal{L}_{\pi(K)}/(\mathcal{L}_{\pi} + \mathcal{L}_K)$ , where  $\mathcal{L}_{\pi(K)}$  denotes the product of each  $\pi(K)$  likelihood of their energy loss ( $dE/dx$ ) in the central drift chamber and their Čerenkov light yield in the ACC. Each likelihood is calculated from a PDF determined using MC simulation. The PID efficiency and fake rate are measured using  $\pi$  and  $K$  tracks in the same kinematic range as signal, with kinematically selected  $D^{*+} \rightarrow D^0\pi^+$ ,  $D^0 \rightarrow K^-\pi^+$  decays. The efficiency and fake rate for  $\pi$  mesons are measured to be 92% and 4% (true  $\pi$  fakes  $K$ ), whereas those for  $K$  mesons are 85% and 10% (true  $K$  fakes  $\pi$ ), respectively. The relative systematic error in the PID efficiency is 2.5% per charged  $\pi$  or  $K$  meson.

Figure 1 shows the  $m_{bc}$  and  $\Delta E$  distributions in the signal region of the other variable, for the  $\pi^+\pi^-$ ,  $K^+\pi^-$  and  $K_S^0\pi^+$  modes. Each  $m_{bc}$  and  $\Delta E$  distribution is fitted to a Gaussian signal plus a background function. The  $m_{bc}$  and  $\Delta E$  peak positions and  $m_{bc}$  width are calibrated using the  $B^+ \rightarrow \bar{D}^0\pi^+$ ,  $\bar{D}^0 \rightarrow K^+\pi^-$  data sample. The  $\Delta E$  Gaussian width is calibrated using high momentum  $D^0 \rightarrow K^-\pi^+$  and  $D^+ \rightarrow K_S^0\pi^+$  decays. The  $m_{bc}$  background shape is modeled by the ARGUS background function [11] with parameters determined using positive  $\Delta E$  sideband data. A linear function is used to model the shape of the  $\Delta E$  background; the slope is fixed at the value determined from the  $m_{bc}$  sideband. The signal yields are determined from the  $\Delta E$  fits where there is kinematic separation between the  $h\pi^+$  and  $hK^+$  decays. The  $\pi^+\pi^-$  and  $K^+\pi^-$  fits include a component to account for misidentified backgrounds. The normalizations of these components are free parameters. The extracted yields are listed in Table I. The cross-talk among different signal modes is consistent with expectations based on PID fake rates. No excess is observed in the  $K^+K^-$  and  $K^+K_S^0$  modes.

Figure 2 shows the  $m_{bc}$  and  $\Delta E$  projections for the  $\pi^+\pi^0$ ,  $K^+\pi^0$  and  $K_S^0\pi^0$  modes. For these modes, since the  $\Delta E$  distribution has a long tail, a two-dimensional fit is applied to the  $m_{bc}$  and  $\Delta E$  distributions. The signal distribution is modeled by a smoothed two-dimensional MC histogram, while the background distribution is taken to be the product of the  $m_{bc}$  and  $\Delta E$  background functions discussed above. The signal and background shapes are determined following the same procedure as for the  $h^+h^-$  and  $K_S^0h^+$  modes. The  $\Delta E$  resolution is calibrated using  $D^0 \rightarrow K^-\pi^+\pi^0$  decays where the  $\pi^0$  is reconstructed in the same kinematic range as the signal. For the  $\pi^+\pi^0$  mode, since the cross-talk from  $K^+\pi^0$  is expected to be large and the  $\Delta E$  separation is less than  $1\sigma$ , the  $K^+\pi^0$  component is fixed at its expected level. The obtained yields are listed in Table I.

The systematic error in the signal yield is determined by varying the parameters of the fitting functions within  $\pm 1\sigma$  of their nominal values. The changes in the signal yield from

each variation are added in quadrature. These errors range from 1% to 6%. In the  $K^+\pi^-$  mode, the  $\Delta E$  background normalization is influenced by an excess around  $-175$  MeV. In this region, we expect to observe a few background events from  $B$  decays such as  $B \rightarrow \rho\pi$ ,  $K^*\pi$ , and  $K^*\gamma$  (for modes with  $\pi^0$  mesons), based on a MC simulation [12,13] in all signal modes. To estimate their effect, we either exclude the negative  $\Delta E$  sideband from the fit or add these components to the fit based on MC histograms. The resulting change in the signal yield, ranging from 4% to 10%, is added in quadrature to the above systematic error.

Table I summarizes all results. The statistical significance ( $\Sigma$ ) is defined as  $\sqrt{-2 \ln(\mathcal{L}(0)/\mathcal{L}_{\max})}$ , where  $\mathcal{L}_{\max}$  and  $\mathcal{L}(0)$  denote the maximum likelihood with the nominal signal yield and with the signal yield fixed at zero, respectively [12]. The final systematic error is the quadratic sum of the relative error in the signal yield ( $N_s$ ), the reconstruction, PID, and continuum suppression efficiencies, and the number of  $B\bar{B}$  pairs (1%). If  $\Sigma < 3$ , we set a 90% confidence level upper limit on the signal yield ( $N_s^{\text{U.L.}}$ ) from the relation  $\int_0^{N_s^{\text{U.L.}}} \mathcal{L}(N_s) dN_s / \int_0^\infty \mathcal{L}(N_s) dN_s = 0.9$ , where  $\mathcal{L}(N_s)$  denotes the maximum likelihood with the signal yield fixed at  $N_s$ . The branching fraction upper limit (U.L.) is then calculated by increasing  $N_s^{\text{U.L.}}$  and reducing the efficiency by their systematic errors.

In summary, using 11.1 million  $B\bar{B}$  events recorded in the Belle detector, the charge averaged branching fractions for  $B \rightarrow \pi^+\pi^-$ ,  $K^+\pi^-$ ,  $K^+\pi^0$ ,  $K^0\pi^+$ , and  $K^0\pi^0$  are measured with statistically significant signals. For the  $\pi^+\pi^0$  mode, an excess is seen with marginal significance. No excess is observed for the  $K^+K^-$  and  $K^+\bar{K}^0$  modes. For these modes, 90% confidence level upper limits are set. The results are listed in Table I. In Table II, we list some ratios of branching fractions based on these measurements. Recent theoretical work [1] suggests that the ratio  $\mathcal{B}(B^+ \rightarrow \pi^+\pi^0)/\mathcal{B}(B^0 \rightarrow \pi^+\pi^-)$  is relevant for extracting  $\phi_2$ , the ratio  $\mathcal{B}(B^+ \rightarrow K^+\pi^0)/\mathcal{B}(B^0 \rightarrow K^+\pi^-)$  is relevant for determining the contribution from electro-weak penguins, and the remaining four ratios are useful to constrain  $\phi_3$ . All the branching fraction and ratio results are consistent with other measurements [2,4]. Our results confirm that  $\mathcal{B}(B^0 \rightarrow K^+\pi^-)$  is larger than  $\mathcal{B}(B^0 \rightarrow \pi^+\pi^-)$ , and indicate that  $\mathcal{B}(B^+ \rightarrow h^+\pi^0)$  and  $\mathcal{B}(B^0 \rightarrow K^0\pi^0)$  seem to be larger than expected in relation to the  $B^0 \rightarrow h^+\pi^-$  and  $B^+ \rightarrow K^0\pi^+$  modes based on isospin or penguin dominance arguments [1].

We wish to thank the KEKB accelerator group for the excellent operation of the KEKB accelerator. We acknowledge support from the Ministry of Education, Culture, Sports, Science, and Technology of Japan and the Japan Society for the Promotion of Science; the Australian Research Council and the Australian Department of Industry, Science and Resources; the Department of Science and Technology of India; the BK21 program of the Ministry of Education of Korea and the CHEP SRC program of the Korea Science and Engineering Foundation; the Polish State Committee for Scientific Research under contract No.2P03B 17017; the Ministry of Science and Technology of Russian Federation; the National Science Council and the Ministry of Education of Taiwan; the Japan-Taiwan Cooperative

## References

- [1] For theory discussions, see for example: A.J. Buras and R. Fleischer, *Eur. Phys. J.* **C16**, 97 (2000); M. Neubert, *Nucl. Phys. Proc. Suppl.* **99**, 113-120 (2001); J. Rosner, in *Lecture Notes TASI-2000*, World Scientific (2001); Y.Y. Keum, H.N. Li, A.I. Sanda, *Phys. Rev.* **D63**, 054008 (2001).
- [2] CLEO Collaboration, D. Cronin-Hennessy *et al.*, *Phys. Rev. Lett* **85**, 515 (2000).
- [3] Belle Collaboration, P. Chang, in *Proc. 30th Int. Conf. on High Energy Phys. (ICHEP)*, edited by C.S. Lim and T. Yamanaka, World Scientific (2001).
- [4] BABAR Collaboration, T. Champion, in *Proc. 30th ICHEP*, edited by C.S. Lim and T. Yamanaka, World Scientific (2001).
- [5] Belle Collaboration, K. Abe *et al.*, KEK Progress Report 2000-4 (2000), to be published in *Nucl. Inst. and Meth. A*.
- [6] KEKB B Factory Design Report, KEK Report 95-7 (1995), unpublished.
- [7] R. Brun *et al.*, GEANT 3.21, CERN Report No. DD/EE/84-1 (1987).
- [8] G. Fox and S. Wolfram, *Phys. Rev. Lett* **41**, 1581 (1978).
- [9] R.A. Fisher, *Annals of Eugenics*, **7**, 179 (1936).
- [10] The Super Fox-Wolfram was first proposed as an extension of  $R_2$  in a series of lectures on continuum suppression at KEK by R. Enomoto in May and June, 1999.
- [11] H. Albrecht *et al.*, *Phys. Lett. B* **241**, 278 (1990).
- [12] Particle Data Group, D.E. Groom *et al.*, *Eur. Phys. J.* **C15**, 1 (2000).
- [13] CLEO Collaboration, D. Cinabro, in *Proc. 30th ICHEP*, edited by C.S. Lim and T. Yamanaka, World Scientific (2001); CLEO Collaboration, R. Stroynowski, *ibid.*



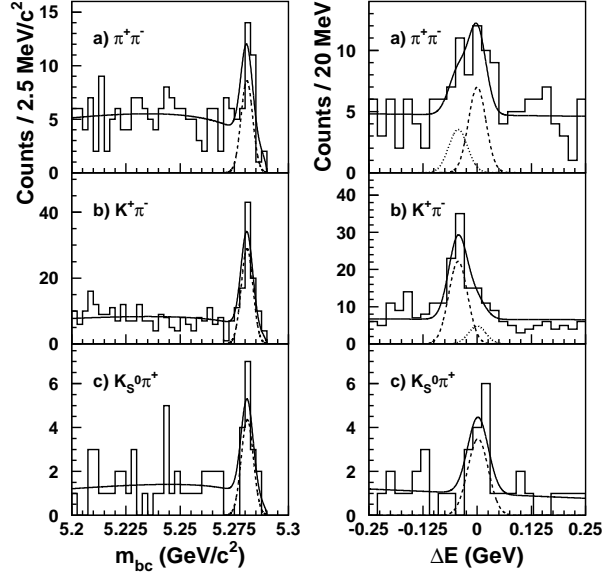


FIG. 1. The  $m_{bc}$  (left) and  $\Delta E$  (right) distributions, in the signal region of the other variable, for  $B \rightarrow$  a)  $\pi^+\pi^-$ , b)  $K^+\pi^-$  and c)  $K_S^0\pi^+$ . The fit function and its signal component are shown by the solid and dashed curve, respectively. In the  $\pi^+\pi^-$  and  $K^+\pi^-$  fits, the cross-talk components are shown by dotted curves.

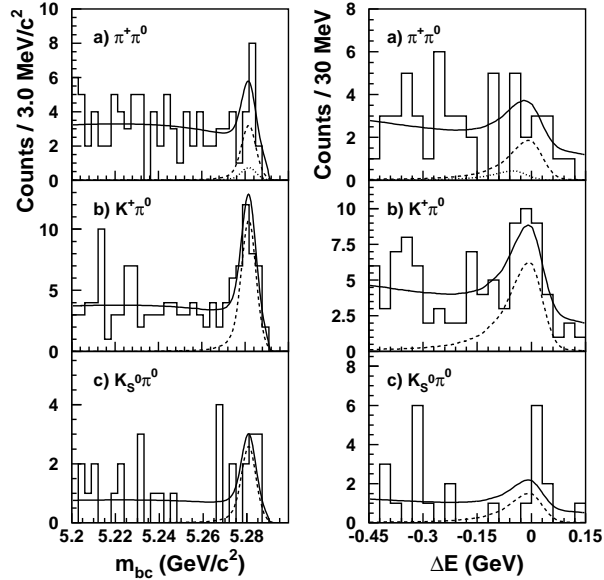


FIG. 2. The  $m_{bc}$  (left) and  $\Delta E$  (right) projections for  $B \rightarrow$  a)  $\pi^+\pi^0$ , b)  $K^+\pi^0$  and c)  $K_S^0\pi^0$ . For  $K^+\pi^0$ , a  $K$  mass is assumed for the charged particle. The projection of the two-dimensional fit onto each variable and its signal component are shown by the solid and dashed curve, respectively. In the  $\pi^+\pi^0$  fit, the cross-talk from  $K^+\pi^0$  is indicated by a dotted curve.

TABLE I. Summary of the results. The obtained signal yield ( $N_s$ ), statistical significance ( $\Sigma$ ), efficiency ( $\epsilon$ ), charge averaged branching fraction ( $\mathcal{B}$ ) and its 90% confidence level upper limit (U.L.) are shown. In the calculation of  $\mathcal{B}$ , the production rates of  $B^+B^-$  and  $B^0\overline{B}^0$  pairs are assumed to be equal. In the modes with  $K^0$  mesons,  $N_s$  and  $\epsilon$  are quoted for  $K_S^0$ , while  $\mathcal{B}$  and U.L. are for  $K^0$ . Submode branching fractions for  $K_S^0 \rightarrow \pi^+\pi^-$  and  $\pi^0 \rightarrow \gamma\gamma$  are included in  $\epsilon$ . The first and second errors in  $N_s$  and  $\mathcal{B}$  are statistical and systematic errors, respectively.

Mode	$N_s$	$\Sigma$	$\epsilon$ [%]	$\mathcal{B} [\times 10^{-5}]$	U.L. [ $\times 10^{-5}$ ]
$B^0 \rightarrow \pi^+\pi^-$	17.7 $^{+7.1}_{-6.4}$ $^{+0.3}_{-1.1}$	3.1	28.1	0.56 $^{+0.23}_{-0.20} \pm 0.04$	–
$B^+ \rightarrow \pi^+\pi^0$	10.4 $^{+5.1}_{-4.3}$ $^{+1.2}_{-1.6}$	2.7	12.0	0.78 $^{+0.38}_{-0.32}$ $^{+0.08}_{-0.12}$	1.34
$B^0 \rightarrow K^+\pi^-$	60.3 $^{+10.6}_{-9.9}$ $^{+2.7}_{-1.1}$	7.8	28.0	1.93 $^{+0.34}_{-0.32}$ $^{+0.15}_{-0.06}$	–
$B^+ \rightarrow K^+\pi^0$	34.9 $^{+7.6}_{-7.0}$ $^{+0.6}_{-2.0}$	7.2	19.2	1.63 $^{+0.35}_{-0.33}$ $^{+0.16}_{-0.18}$	–
$B^+ \rightarrow K^0\pi^+$	10.3 $^{+4.3}_{-3.6}$ $^{+0.4}_{-0.1}$	3.5	13.5	1.37 $^{+0.57}_{-0.48}$ $^{+0.19}_{-0.18}$	–
$B^0 \rightarrow K^0\pi^0$	8.4 $^{+3.8}_{-3.1}$ $^{+0.4}_{-0.6}$	3.9	9.4	1.60 $^{+0.72}_{-0.59}$ $^{+0.25}_{-0.27}$	–
$B^0 \rightarrow K^+K^-$	0.2 $^{+3.8}_{-0.2}$	–	24.0	–	0.27
$B^+ \rightarrow K^+\overline{K}^0$	0.0 $^{+0.9}_{-0.0}$	–	12.1	–	0.50

TABLE II. Ratio of charge averaged branching fractions ( $\mathcal{B}$ ) for  $B \rightarrow \pi\pi$ , and  $K\pi$  decays. The first error is statistical and the second is systematic. The correlation and cancellation of systematic errors are taken into account. A 90% confidence level upper limit in the first ratio, is calculated using a similar method as the upper limit of  $\mathcal{B}$  described in text.

Modes	Ratio
$\mathcal{B}(B^+ \rightarrow \pi^+\pi^0)/\mathcal{B}(B^0 \rightarrow \pi^+\pi^-)$	< 2.67
$2\mathcal{B}(B^+ \rightarrow K^+\pi^0)/\mathcal{B}(B^0 \rightarrow K^+\pi^-)$	1.69 $^{+0.46}_{-0.45}$ $^{+0.17}_{-0.19}$
$\mathcal{B}(B^0 \rightarrow \pi^+\pi^-)/\mathcal{B}(B^0 \rightarrow K^+\pi^-)$	0.29 $^{+0.13}_{-0.12}$ $^{+0.01}_{-0.02}$
$\mathcal{B}(B^0 \rightarrow K^+\pi^-)/2\mathcal{B}(B^0 \rightarrow K^0\pi^0)$	0.60 $^{+0.25}_{-0.29}$ $^{+0.11}_{-0.16}$
$2\mathcal{B}(B^+ \rightarrow K^+\pi^0)/\mathcal{B}(B^+ \rightarrow K^0\pi^+)$	2.38 $^{+0.98}_{-1.10}$ $^{+0.39}_{-0.26}$
$\mathcal{B}(B^0 \rightarrow K^+\pi^-)/\mathcal{B}(B^+ \rightarrow K^0\pi^+)$	1.41 $^{+0.55}_{-0.63}$ $^{+0.22}_{-0.20}$